scientific reports

Check for updates

OPEN

Insights into novel konjac glucomannan/zein/fatty acid composite films with excellent properties for food packaging

Xiumei Wang[1,2,3], Xiaoyan Zheng[1], Leqian Chu[1], Xiaoxu Zhao[2]✉ & Jie Pang[4]✉

Conventional non-degradable petroleum-based packaging films cause serious food safety and white environment pollution problems. Thus, a series of novel konjac glucomannan (KGM)/zein (KZ) films with different chain lengths and concentrations of fatty acids were prepared using a solution casting method in this paper. Effects of stearic acid and lauric acid on the rheological properties of the film-forming solutions, structure, mechanical properties and water barrier abilities of KZ film were systematically studied. The apparent viscosities analysis indicated that all the film-forming solutions were typical non-Newtonian pseudoplastic fluids and KGM/Zein/fatty acid (KZ-FA) film solutions exhibited higher apparent viscosities than KZ film solution at the test FA concentration. Fourier transform infrared spectroscopy results confirmed that hydrogen bonds were the main intermolecular interactions among KGM, Zein and fatty acids. Differential scanning calorimetry and X-ray diffraction results demonstrated that the incorporation of fatty acids enhanced the thermal stabilities and crystallinities of KZ film. Scanning electron microscopy and atomic force microscope results revealed that the surface morphologies and roughness of KZ film were significantly affected after adding FAs. The rougher and more irregular surfaces were observed in the KZ films with stearic acid. Moreover, KZ film with 0.4% stearic acid exhibited higher surface hydrophobicity, mechanical, water resistance and water vapor barrier properties than other KGM-based films. These results suggested that KZ films with appropriate types and concentrations of fatty acids are promising food packaging films for the required properties.

Keywords Konjac glucomannan, Zein, Fatty acids, Composite film, Structure, Properties

Recently, food packaging films prepared from various natural polymers such as lipids, proteins, and polysaccharides have drawn great attention due to their biodegradability and non-toxic properties[1–5]. Among these natural biodegradable polymers, konjac glucomannan (KGM), a water-soluble natural and renewable macromolecular polysaccharide with molecular chains consisting of D-glucose and D-mannose linked by β-1,4-glycosidic bonds, is an ideal candidate for the production of food packaging films because of its high availability, low cost, beneficial bioactivity, excellent film-forming ability, high hydrophilicity, non-toxicity, good biocompatibility and biodegradability[6–8]. However, pure KGM film has poor thermal stability, low mechanical strength and high water sensitivity, limiting its widespread applications in various fields[9–11].

An effective method to enhance the performances of pure KGM film is to incorporate other biodegradable film-forming components[12,13]. Zein, a natural polymer, has been widely used to prepare food packaging films due to its good film-forming ability, strong hydrophobic characteristic and excellent oxygen barrier property[14–17]. Studies have showed that the addition of zein could improve the thermal stability, mechanical and hydrophobic properties of pure KGM film[18–20]. However, the water vapor barrier properties of KGM/Zein film still can't meet the current requirements of food packaging films and need to be further enhanced[21]. Therefore, it is necessary to further look for higher hydrophobic constituents for the preparation of biodegradable composite films with better moisture barrier properties.

[1]College of Environmental and Biological Engineering, Putian University, Putian 351100, China. [2]Fujian Provincial Key Laboratory of Ecological Impacts and Treatment Technologies for Emerging Contaminants, Putian University, Putian 351100, China. [3]Key Laboratory of Ecological Environment and Information Atlas of Fujian Provincial University, Putian University, Putian 351100, China. [4]College of Food Science, Fujian Agriculture and Forestry University, Fuzhou 350002, China. ✉email: zhaoxiaoxu0711@126.com; pang3721941@163.com

Nowadays, fatty acids are becoming more and more attractive in the field of food packaging films due to their high hydrophobicity[22,23]. Many studies have indicated that incorporating fatty acids such as lauric acid (LA), palmitic acid and stearic acid (SA) could enhance the water vapor barrier properties of various films[24–27]. Although there are many works about food packaging films containing fatty acids[28,29], it is still unknown whether the effects of different fatty acids on the structure and properties of different composite films are similar. Moreover, there are no reports available on the structure and properties of KGM/Zein films with fatty acids. Considering that unsaturated fatty acids are prone to oxidation and excessive temperatures may cause protein denaturation, saturated fatty acids were selected in this paper[22,30]. Among the saturated fatty acids, LA and SA were widely used as hydrophobic additive in food packaging films formulations due to their classification as generally recognized as safe (GRAS) by the Food and Drug Administration (FDA), mild melting temperatures (c.a, 44 ℃ for LA and 72 ℃ for SA), good biodegradability, rich source and low cost[22,29,30]. Therefore, the aim of this paper was to investigate the effects of LA and SA on the properties and structure of KGM/Zein film. Firstly, a solution casting method was employed to develop novel hydrophobic composite films by incorporating different concentrations of LA and SA into KGM/Zein film. Subsequently, the physicochemical properties analysis and structural characterization of KGM/Zein/fatty acid composite films were carried out. Finally, the underlying mechanism of incorporating fatty acids into KGM/Zein film was discussed.

Materials and methods

Materials

Lauric acid (98%) was sourced from Shanghai Maclean's Biochemical Technology Co., Ltd. (Shanghai, China). Konjac glucomannan (≥ 95% purity), zein, anhydrous calcium chloride and stearic acid (98%) were obtained from Shanghai Aladdin Biochemical Technology Co., Ltd. (Shanghai, China). Glycerol and anhydrous ethanol were purchased from China National Pharmaceutical Group Chemical Reagent Co., Ltd. (Shanghai, China). All other reagents were of analytical grade unless otherwise stated.

Preparation of KGM/Zein/fatty acid films

Pure KGM film solution was gained by dissolving 0.75 g KGM and 0.05 g glycerol in 100 mL of distilled water with continuous stirring at 70 ℃ for 1 h. The preparation of pure Zein film solution was carried out under the conditions of 2 g zein, 1 g glycerol and 100 mL of 80% ethanol aqueous solution at 35 ℃ for 30 min. Subsequently, pure KGM and Zein film solutions with the volume ratio of 10:1 were blended at 70 ℃ for 30 min in order to obtain KGM/Zein film solution. Afterwards, KGM/Zein/fatty acid film solutions were prepared by incorporating SA (0.1, 0.2, 0.3, 0.4, 0.5 and 0.6% pure KGM film solution) or LA (0.04, 0.05, 0.06, 0.07, 0.08 and 0.09% pure KGM film solution) into KGM/Zein film solution at 70 ℃ with 1 h-stirring. Finally, all the obtained films after drying at 60 ℃ for 6 h were peeled off and equilibrated at room temperature and 50% relative humidity in a constant temperature and humidity box before use. The above films were sequentially coded as KGM, Zein, KZ, KZS_1, KZS_2, KZS_3, KZS_4, KZS_5, KZS_6, KZL_4, KZL_5, KZL_6, KZL_7, KZL_8 and KZL_9, respectively.

Apparent viscosities of various film solutions

A Hack Rheometer (Viscotester iQ, Hack Corporation, Kurtscheid, Germany) containing FL 22 4B/SS-01160184 rotor was employed to measure the apparent viscosities of various film solutions at 25 ℃. The rotor speed and measurement time were set to 65 r/s and 30 s, respectively. One point was measured every 2 s during this period.

Fourier transform infrared spectroscopy (FTIR) analysis of various films

Various films were cut into 2 cm×2 cm prior to use. Then, the FTIR measurements of various films were performed using a TENOSOR27 FTIR spectrometer (Burker Corporation, North Billerica, MA, USA). The scanning wavelength range, resolution and number were 400–4000 cm^{-1}, 4 cm^{-1} and 32 times, respectively.

X-ray diffraction (XRD) analysis of various films

Various films were trimmed to small discs with a diameter of 4 cm before use. Then, the crystalline characterisitics of various films were analyzed by an X-ray diffractometer (XRD-6100, Shimadzu Corporation, Kyoto, Japan). The analysis was carried out at a voltage of 40 kV and a current of 30 mA with Cu-Kα radiation source. The scanning speed and angular range were 2°/min and 5–40° (2θ), respectively.

Thermal stabilities of various films

Various films were first tailored to small pieces and then were sealed in the aluminum pans. After that, the thermal properties of various films were analyzed under a nitrogen (N_2) atmosphere using a NETZSCH DSC 214 (Netzsch Co, Selb, Bavaria, Germany) from 35 to 200 ℃ at a heating rate of 10 ℃/min.

Surface morphologies analysis of various films

The surface morphologies of various films were analyzed by scanning electron microscopy (SEM) (SU-8010, Hitachi Ltd., Tokyo, Japan). Before the analysis, various films were trimmed to small pieces with the size of 1 cm×1 cm. Then, these pieces were pasted onto the sample stage with a double-sided adhesive tape and sputtered under vacuum with gold for SEM analysis. During the analysis process, the accelerating voltage and magnification were set to 10 kV and 1000-fold, respectively.

Atomic force microscope (AFM) analysis of various films

Before the analysis, various films were cropped to a square (5 mm×5 mm) and then fixed on the sample table. After that, an atomic force microscope (AFM) (Bruker Dimension ICON, Bruker, Germany) was employed to observe the surface roughness of various films. All AFM images were obtained in tapping mode at room

temperature. The roughness parameters of various films such as root-mean-square roughness (Rq) and average roughness (Ra) were analysis using NanoScope software version 5.31.

Mechanical properties of various films

Before the measurement, various films were cropped to long strips (20 mm×80 mm). Then, the thicknesses of these strips were tested using a spiral micrometer (DL9325, Deli Group Co., Ltd, Ningbo, China). After that, the mechanical properties of various films were measured by a CT3-4500 Texture Analyzer (Ametek Corporation, Berwyn, PA, United States) under the conditions of a trigger point load of 0.1 N, a speed of 0.5 mm/s and an initial grip length of 50 mm. The elongation at break (EB, %) and tensile strength (TS, MPa) values of various films were calculated using the equations listed below (Eqs. 1 and 2), respectively.

$$EB = \frac{L - L_0}{L_0} \times 100 \tag{1}$$

$$TS = \frac{F}{W \times \mathrm{T}} \tag{2}$$

where F (N), T (mm), W (mm), L_0 (mm) and L (mm) mean the maximum force, the thickness, width, the original and final lengths of various films, respectively.

Water vapor permeability (WVP) of various films

The WVP measurements of various films were carried out according to the previous reports[31,32] with a slight modification. Firstly, anhydrous calcium chloride (3 g) after drying at 105 ℃ for 6 h was added into the glass cups. Then, the glass cups were sealed by various films, weighed and placed in a constant temperature and humidity box. The temperature and relative humidity were 25 ℃ and 90%, respectively. During the measurements, the glass cups were weighed every 1 h until the weight change was less than 5%. The WVP values ($g{\cdot}m^{-1}{\cdot}s^{-1}{\cdot}Pa^{-1}$) of various films were calculated by the following equation (Eq. 3).

$$WVP = \frac{\Delta m \times \mathrm{T}}{S \times \Delta t \times \Delta P} \tag{3}$$

where $\Delta m/\Delta t$ ($g{\cdot}s^{-1}$) and ΔP (Pa) represent the weight change of the glass cups versus time and the water vapor pressure difference between two sides of various films, respectively; S (m^2) and T (m) represent the effective area and thickness of various films, respectively.

Water solubility (WS) of various films

Various films (2 cm×2 cm) after drying at 105 ℃ in an oven for 24 h were directly immersed in distilled water (30 mL) at room temperature for 24 h. Then, various insoluble films were collected and dried again at 105 ℃ in an oven until the weight reached a constant value. The WS values of various films were calculated by the following equation (Eq. 4).

$$WS\,(\%) = \frac{m_1 - m_2}{m_1} \times 100 \tag{4}$$

where m_1 (g) represents the weight of various films before the immersion, m_2 (g) represents the weight of various films after immersing and drying.

Water contact angle (WCA) of various films

The WCA analysis of various films was carried out using a fully automatic contact angle measuring instrument (SL250, KINO Scientifc Instrument Inc., Boston, MA, USA) with the sessile drop method at room temperature. Before the analysis, various films were cropped to a rectangle (10 mm×20 mm) and pasted onto the sample stage with adhesive tape. Then, a total of 10 μL of distilled water was dropped on the surfaces of various films using a microsyringe. After the droplets stabilized, photos were captured and the Young-Laplace equation was employed to calculate the WCA values of various films.

Statistical analysis

All the assays were conducted three times and the related results were presented as the means ± standard deviations (SD). The analysis of statistical data was carried out using SPSS 26 software and Origin 8.0 software. The difference of the experimental data ($P < 0.05$) was determined using Duncan's multiple range tests, the analysis of variance, and Least significant differences (LSD) multiple comparison tests.

Results and discussion

Apparent viscosities of various film solutions

The effects of fatty acids on the apparent viscosities of KZ film solution are presented in Fig. 1. As seen from Fig. 1, KZ and KZ-FA film solutions had significantly lower viscosities than pure KGM film solution. This may be probably because the formation of KGM gel was destroyed and new hydrogen bond interactions were formed among KGM, Zein and/or fatty acids. It was also found that the viscosities of KZ-FA film solutions were higher than that of KZ film solution, indicating that the entanglement network of KGM and zein had been embedded by fatty acids. In addition, the viscosities of KZ-FA film solutions were discovered to decrease as FA concentrations increased. This may be probably because adding fatty acids to KZ film solution reduced solvent quality and

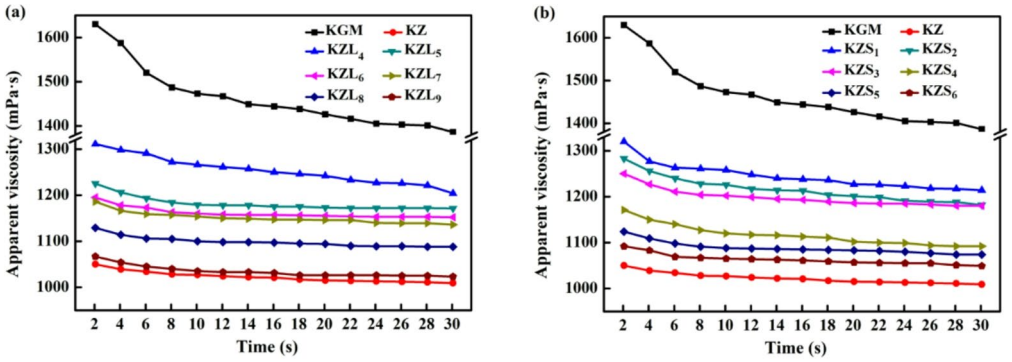

Fig. 1. Rheological properties of various film solutions. (**a**) Pure KGM, KZ and KZL film solutions; (**b**) Pure KGM, KZ and KZS film solutions.

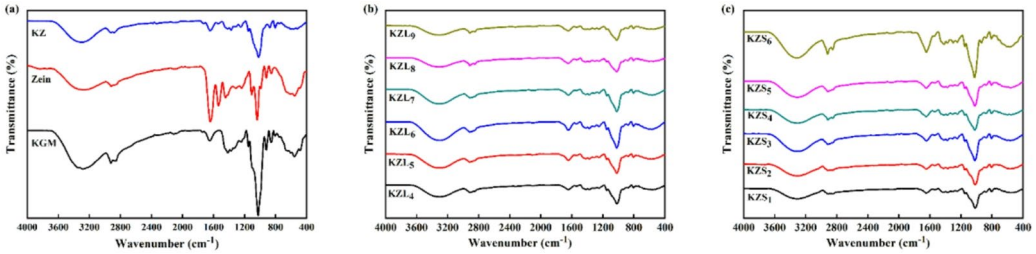

Fig. 2. FTIR results. (**a**) Pure KGM, Zein and KZ films; (**b**) KZL films; (**c**) KZS films.

destroyed the hydrogen bonds between KGM and zein. However, the viscosities of all the film solutions decreased as the shear time increased, suggesting a shear-thinning behavior. The primary reason for this was that polymer chains were decomposed and rearranged under shear force[33,34]. Moreover, incorporating different fatty acids did not cause much change in the viscosity of KZ film solution. These results indicated that adding fatty acids could enhance the viscosity of KZ film solution.

FTIR analysis of various films

The effects of fatty acids on the functional groups of KZ film are shown in Fig. 2. It was observed that the stretching vibration absorption bands of -OH, -CH_2 and -CH bonds in pure KGM film appeared at 3286, 2925 and 2866 cm^{-1}, respectively. In addition, the peaks at 1644 and 1024 cm^{-1} in the spectrum of pure KGM film were ascribed to intramolecular hydrogen bonds and C-O-C groups, respectively. The peaks at 855 and 804 cm^{-1} were caused by mannose unit stretching vibration in KGM[21,35]. The spectrum of pure Zein film showed characteristic absorption peaks at 3284 cm^{-1} (N-H stretching vibration), 1641 cm^{-1} (C = O stretching vibration in the amide I), 1535 cm^{-1} (N-H bending vibration in the amide II), 1444 cm^{-1} (–CH_2 bending vibration), 1037 cm^{-1} (C-N stretching vibration in the amide III), respectively. Moreover, the absorption peaks of C-H stretching vibration in the aliphatic groups of pure Zein film occurred at 2917 and 2850 cm^{-1}[19].

It was also found that KZ, KZL and KZS films had all characteristic absorption peaks of pure KGM and Zein films. Moreover, no new absorption peaks were discovered in the spectra of these composite films, indicating that there were no chemical reactions occurring during the preparation processes of KZ, KZL and KZS films. However, compared to KZ film, the absorption peak of hydroxyl group stretching vibration significantly shifted from 3296 to 3309 cm^{-1} and 3306 cm^{-1} with increased intensity after adding LA and SA, respectively. This indicated that hydrogen bonds were formed among KGM, zein and fatty acids. Moreover, the intensities of the characteristic absorption peaks at around 2917 and 2847 cm^{-1} in the spectra of KZ-FA films increased as the concentrations of FA increased. It could be concluded that the addition of fatty acids had no significant influence on the structure of KZ film, but hydrogen bond interactions among KGM, zein and fatty acids may result in better water vapor barrier and mechanical properties.

XRD analysis of various films

Figure 3 shows the XRD patterns of KGM, Zein, KZ and KZ films with different types and concentrations of fatty acids. The pure KGM film exhibited a broad characteristic diffraction peak at 2θ = 20.3°, demonstrating that KGM was an amorphous substance. Similar results were observed in the previous literatures[19,36–38]. In addition, the XRD pattern of pure Zein film appeared two diffraction peaks at 2θ = 8.9° and 20.5°, which was in agreement with the previous results[30,39]. After adding zein to pure KGM film, the diffraction peak at 2θ = 9.3° disappeared. Moreover, the wide peak intensity of KZ film at 2θ = 20.3° decreased compared to pure KGM film. This may

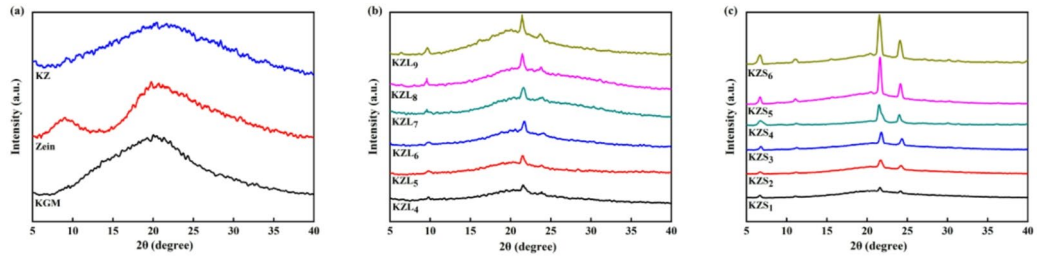

Fig. 3. XRD results. (**a**) Pure KGM, Zein and KZ films; (**b**) KZL films; (**c**) KZS films.

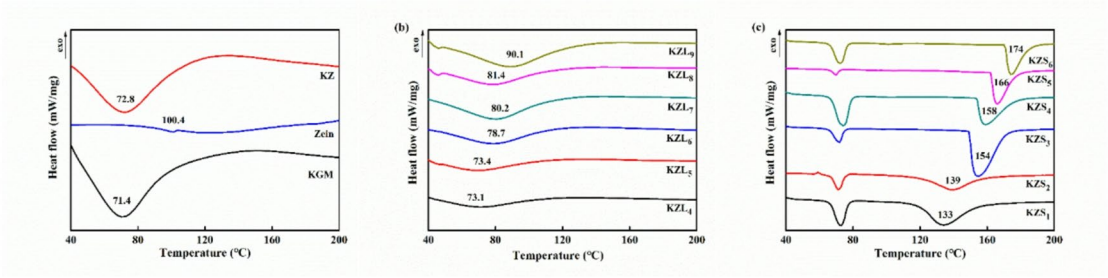

Fig. 4. DSC results. (**a**) Pure KGM, Zein and KZ films; (**b**) KZL films; (**c**) KZS films.

be due to the good compatibility and intermolecular hydrogen bonds between KGM and zein in the composite film[21].

After further incorporating fatty acids into KZ film, the peak at 2θ = 20.3° disappeared. This may be probably because fatty acids formed intermolecular hydrogen bonds with KGM and/or zein molecules, reducing crystal growth and forming the most stable structure by interfering with the arrangement of polymer chains[22,40]. However, four new characteristic diffraction peaks at 2θ = 6.7°, 11°, 21.5° and 24.1° appeared in the spectra of KZS films, and three new characteristic diffraction peaks at 2θ = 9.7°, 21.5° and 23.8° emerged in the spectra of KZL films, which corresponded to the characteristic diffraction peaks of SA and LA, respectively[22]. Meanwhile, the intensities of these new characteristic diffraction peaks in the spectra of KZS and KZL films increased with the increase of FA concentrations. It was possible that an ordered molecular arrangement of fatty acids was formed in the composite films[41]. It could be concluded that KZS and KZL films had the highest crystallinities when SA and LA concentrations were 0.6% and 0.09%, respectively. Therefore, incorporating fatty acids into KZ film could effectively enhance their crystallinities.

DSC analysis of various films

The effects of fatty acids on the thermal properties of KZ film are displayed in Fig. 4. It could be seen from Fig. 4 that the DSC curves of pure KGM and KZ films presented only one endothermic peak at 71.4 and 72.8 ℃, respectively, which corresponded to the respective glass transition temperature (Tg). This result indicated that KZ film had higher thermal stability than pure KGM film, which may be ascribed to the good compatibility of KGM and zein molecules and their intermolecular interactions in the composite film[18,21].

As for the DSC curves of KZS and KZL films, the endothermic peaks at around 69 ~ 72 and 44 ℃ were due to the melting points of SA and LA, respectively, which was similar to the previous literatures[22,42]. In addition, it was observed that all the KZS and KZL films presented a single Tg at around 133 ~ 174 and 73 ~ 91 ℃, respectively, indicating good compatibility among KGM, zein and fatty acids. The Tg of KZ-FA films was higher than that of KZ film and shifted gradually to a higher temperature with the increase of FA concentrations. This may be due to the stronger intermolecular interactions in the KZ-FA film matrix with the increase of FA concentrations, resulting in higher thermal stabilities of KZ-FA films. It could be concluded that the thermal stabilities of KZ-FA films showed similar trends as their crystallinities with the increase of FA concentrations. The thermal stabilities of KZS and KZL films reached the maximum when SA and LA concentrations were 0.6% and 0.09%, respectively, as consistent with XRD results. This indicated that the improved crystalline structure required more energy to disrupt, leading to an elevated glass transition temperature. Furthermore, KZS films were discovered to have higher Tg than KZL films, indicating that SA was superior to LA in improving the thermal performances of KZ film. As a result, the incorporation of fatty acids increased the thermal stability of KZ film.

Microstructural analysis of various films

The effects of fatty acids on the surface morphologies of KZ film are shown in Fig. 5. It was observed that the surface of pure KGM film was smooth and uniform, indicating good miscibility between KGM and glycerol,

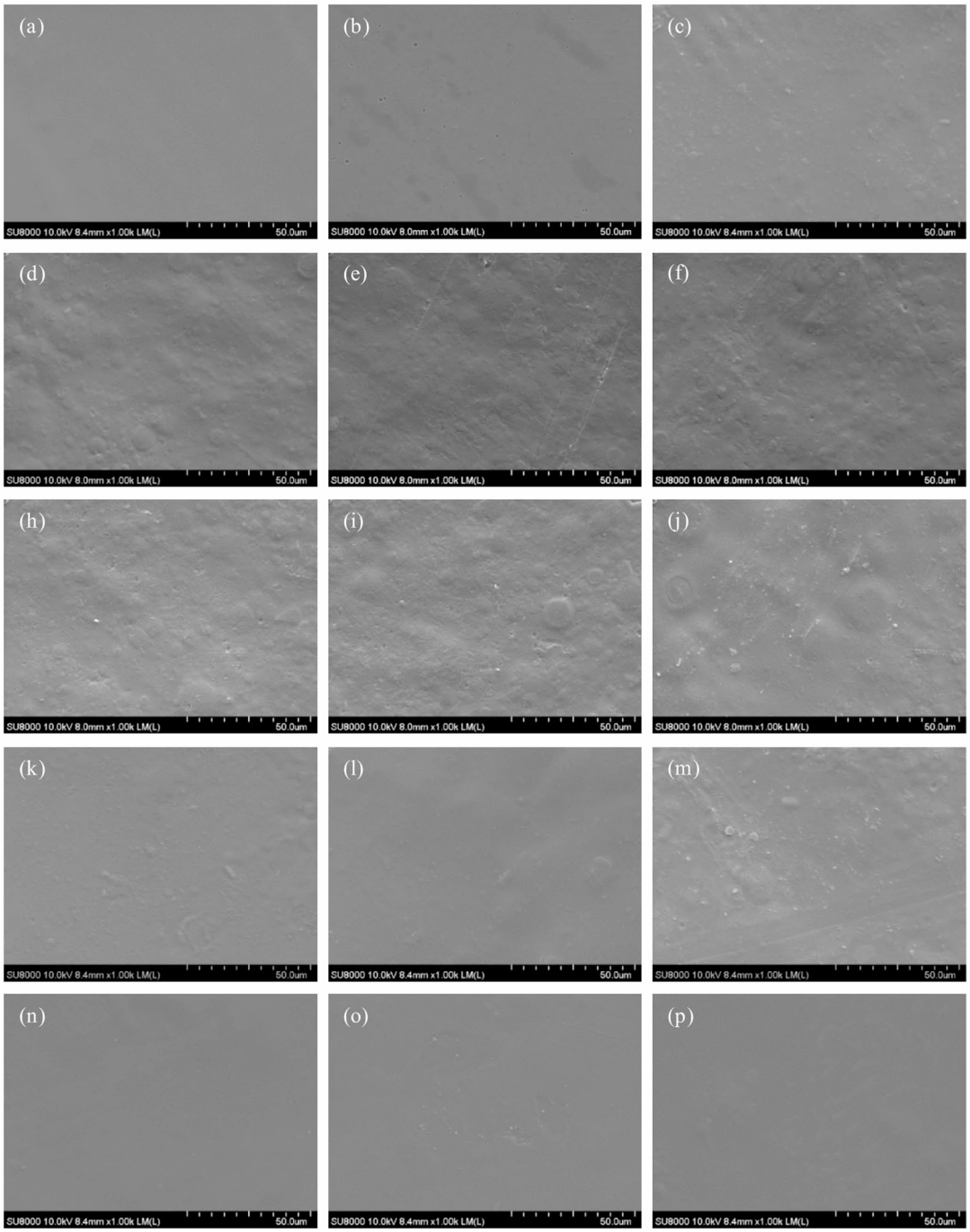

Fig. 5. SEM results. (**a**) Pure KGM film; (**b**) Pure Zein film; (**c**) KZ film; (**d**) KZS_1 film; (**e**) KZS_2 film; (**f**) KZS_3 film; (**g**) KZS_4 film; (**h**) KZS_5 film; (**i**) KZS_6 film; (**j**) KZL_4 film; (**k**) KZL_5 film; (**l**) KZL_6 film; (**m**) KZL_7 film; (**n**) KZL_8 film; (**o**) KZL_9 film.

which was in accordance with the previous reports[33,43]. Pure Zein film showed a relatively smooth surface morphology with black minute pinholes, which may be attributed to the encapsulated air microbubbles[36]. However, KZ film exhibited a little rough surface, which may be due to the intermolecular interactions between KGM and zein in the film matrix[18].

After adding SA to KZ film, a rougher and more irregular structure was observed in the surface of KZS films. This may be related to the agglomerations of the polymers during the preparation progress of KZS films, resulting in the destruction of the network structure formed by KGM and zein. Moreover, the surface roughness and irregularity of KZS films increased first and then decreased with the increase of SA concentrations. When SA concentration was 0.3%, the surface of KZS film was the roughest and most irregular. However, the surface of KZL films presented an irregular trend with the increase of LA concentrations when compared with KZ film. Only KZL_6 film displayed a relatively rougher surface than KZ film. The surfaces of other KZL films were

smoother and more uniform than that of KZ film. When LA concentration was 0.07%, the surface of KZL film was the smoothest and most uniform. This may be ascribed to the high compatibility and intermolecular interactions between LA and KZ film matrix. More importantly, it was found that except for KZS_6 film, the surfaces of other KZS films were rougher and more irregular than those of KZL films. Therefore, it could be concluded that different types and concentrations of fatty acids had great impact on the surface morphologies of KZ film.

Figure 6 shows the effects of fatty acids on the surface roughness of KZ film. It was observed that pure KGM and Zein films had low Ra and Rq values, indicating that their surfaces were relatively smooth and homogenous. Incorporating Zein led to an increase in the surface roughness of pure KGM film. In addition, it was discovered that the Ra and Rq values of KZS films increased first and then decreased as SA concentrations increased, but were higher than those of KZ film, suggesting that KZS films had higher surface roughness than KZ film. KZS film had the highest Ra and Rq values when SA concentration was 0.3%. However, the Ra and Rq values of KZL films exhibited an irregular trend with the increase of LA concentrations. Only KZL_6 film had higher Ra and Rq values than KZ film. The Ra and Rq values of other KZL films were lower than those of KZ film. KZL film had the lowest Ra and Rq values when LA concentration was 0.07%. More importantly, it was found that except for KZS_6 film, other KZS films had higher surface roughness than KZL films. These findings were in accordance

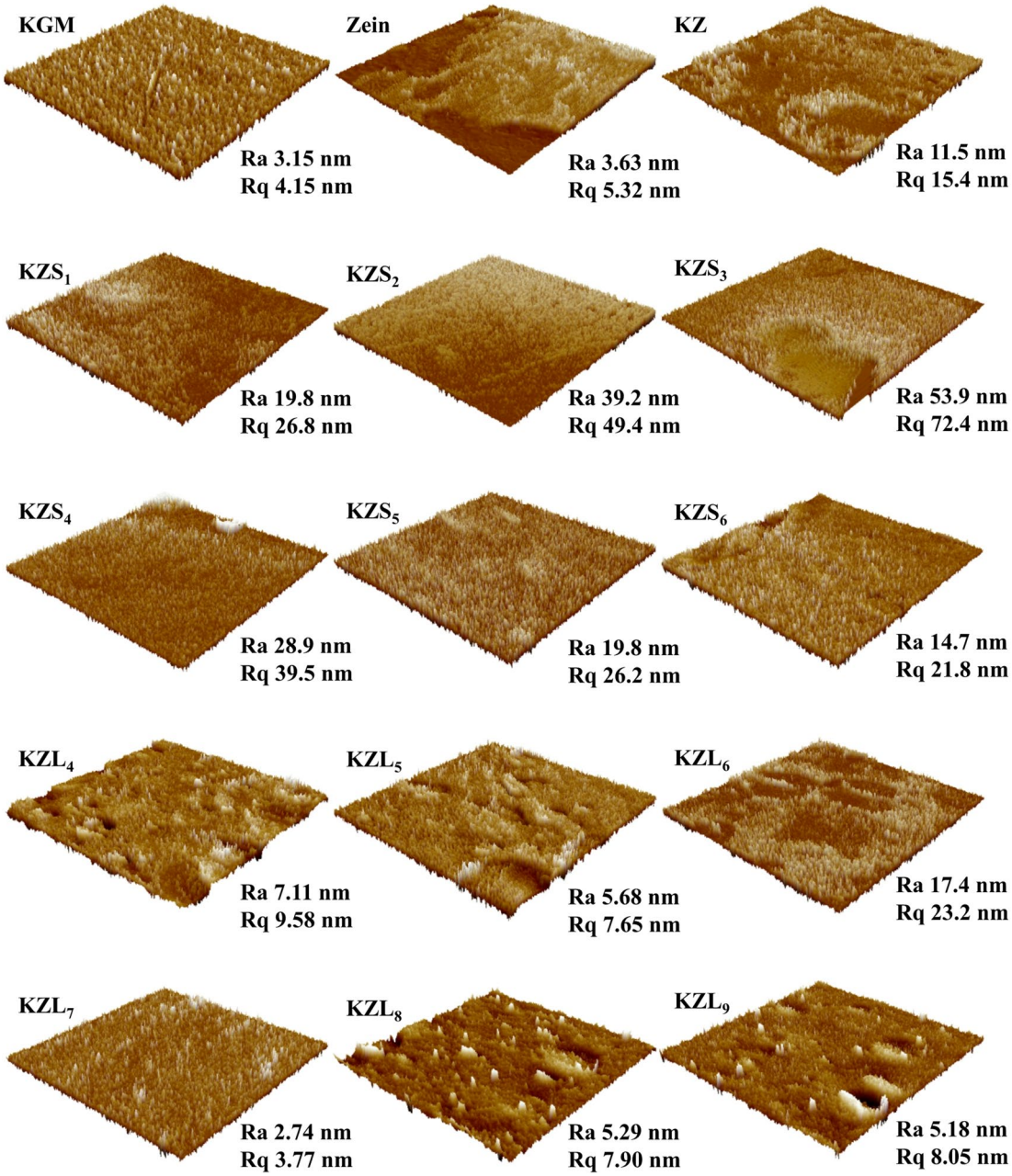

Fig. 6. AFM images of various films.

with those of SEM results. The results indicated that the surface roughness of KZ film was affected by the types and concentrations of fatty acids, as consistent with SEM results.

Mechanical properties of various films

The effects of fatty acids on the mechanical properties of KZ film are shown in Table 1. It was observed that KZ film had higher TS and EB values than pure KGM and Zein films, suggesting that the mechanical properties of pure KGM film were significantly enhanced after adding zein. This may be ascribed to the formation of the compact structure by strong hydrogen bond interactions between KGM and zein molecules[19], as confirmed by FTIR and XRD analysis. In addition, it was found that the TS values of KZ-FA films increased first and then decreased with the increase of FA concentrations. This may be probably because small quantities of fatty acids were uniformly distributed in the films[44], but the uneven distribution of excessive fatty acids weakened intermolecular interactions[45]. Nevertheless, their EB values presented an opposite trend as the concentrations of FA increased. These trends were in agreement with those of soy protein isolate/sodium alginate edible films with fatty acids in the literature[22]. More importantly, it was discovered that KZS_4 film exhibited the highest TS and lowest EB values (30.69 MPa and 2.84%) when compared with other KGM-based films. Furthermore, KZS films exhibited relatively higher TS and lower EB values than KZL films. This may be due to the stronger intermolecular interactions among KGM, zein and SA molecules, resulting in higher mechanical properties. These results demonstrated that incorporating fatty acids with appropriate concentrations could enhance the mechanical properties of KZ film.

WVP, WS and WCA values of various films

The effects of fatty acids on the WVP and WS values of KZ film are shown in Table 2. As seen from Table 2, pure KGM film had poor water vapor barrier properties due to the large number of hydrophilic groups in the KGM molecules[10] and its WVP value reached 9.29×10^{-11} ($g{\cdot}m^{-1}{\cdot}s^{-1}{\cdot}Pa^{-1}$). After adding zein to pure KGM film, the WVP value decreased, which indicated that KZ film had better water vapor barrier properties than pure KGM film due to the intermolecular interactions between KGM and zein containing hydrophobic amino acids[21]. In addition, it was observed that the WVP values of KZ-FA films decreased first and then increased as the concentrations of FA increased. Only KZL_8 and KZL_9 films were discovered to have higher WVP values than KZ film, which meant that only KZL_8 and KZL_9 films had poorer water vapor barrier properties than KZ film. The WVP values of KZS and KZL films reached the minimum values when the concentrations of SA and LA were 0.4% and 0.07%, respectively. This may be probably because the effective path length of water diffusion was enhanced due to the uniform dispersion of a small amount of fatty acids in the hydrophilic phase[46], but the film surface was found to have the discontinuous crystallization and uneven emulsification of fatty acids when an excessive amount of fatty acids was added[47,48]. Moreover, there was no much change in the WVP value of KZ film among different types of fatty acids, which was consistent with the previous reports[22,26,44]. More importantly, it was found that KZS_4 film had the best water vapor barrier properties when compared with other KGM-based films. These results indicated that adding fatty acids with appropriate concentrations to KZ film could be more conductive to food preservation due to better prevention of water loss in food.

The WVP value of the commercial food packaging films was determined to be 1.27×10^{-12} $g{\cdot}m^{-1}{\cdot}s^{-1}{\cdot}Pa^{-1}$, which was lower than those of KZ-FA films. This may be probably because the commercial food packaging films are usually made of specialized non-biodegradable polymer materials such as polyethylene, polyvinyl chloride, or polyvinylidene chloride. In addition, the production processes of commercially available food packaging films may adopt advanced technology such as co extrusion and multi-layer composite, or may undergo surface treatment such as oxidation, which can significantly improve the water vapor barrier performances of the film.

Films	TS (MPa)	EB (%)
KGM	21.10 ± 0.30^{f}	5.98 ± 0.36^{g}
zein	2.78 ± 0.46^{k}	2.56 ± 0.14^{i}
KZ	22.72 ± 0.36^{e}	9.05 ± 0.26^{cd}
KZS_1	19.12 ± 0.23^{g}	9.41 ± 0.32^{bc}
KZS_2	21.14 ± 0.45^{f}	6.88 ± 0.20^{f}
KZS_3	23.21 ± 0.23^{de}	6.28 ± 0.13^{g}
KZS_4	30.69 ± 0.45^{a}	2.84 ± 0.40^{i}
KZS_5	29.22 ± 0.42^{b}	4.10 ± 0.22^{h}
KZS_6	21.22 ± 0.13^{f}	6.98 ± 0.18^{f}
KZL_4	9.90 ± 0.27^{j}	12.58 ± 0.39^{a}
KZL_5	14.65 ± 0.52^{h}	9.70 ± 0.55^{b}
KZL_6	23.72 ± 0.48^{d}	8.26 ± 0.46^{e}
KZL_7	27.34 ± 0.52^{c}	8.22 ± 0.44^{e}
KZL_8	14.14 ± 0.27^{h}	8.60 ± 0.12^{de}
KZL_9	12.92 ± 0.44^{i}	9.62 ± 0.28^{b}

Table 1. Mechanical properties of various films.

Films	WVP×10^{-11} (g·m^{-1}·s^{-1}·Pa^{-1})	WS (%)
KGM	9.29 ± 0.010^{ab}	90.08 ± 0.16^{a}
zein	6.24 ± 0.045^{k}	8.89 ± 0.18^{j}
KZ	9.06 ± 0.025^{c}	35.47 ± 1.48^{d}
KZS_1	8.34 ± 0.025^{ef}	30.10 ± 1.28^{f}
KZS_2	8.10 ± 0.045^{gh}	27.65 ± 0.74^{g}
KZS_3	7.90 ± 0.040^{h}	25.91 ± 0.47^{h}
KZS_4	7.29 ± 0.020^{j}	22.45 ± 0.55^{i}
KZS_5	8.28 ± 0.045^{fg}	29.66 ± 0.67^{f}
KZS_6	8.57 ± 0.040^{de}	32.88 ± 0.07^{e}
KZL_4	8.70 ± 0.035^{d}	34.04 ± 1.37^{de}
KZL_5	8.08 ± 0.060^{gh}	27.84 ± 1.66^{g}
KZL_6	7.56 ± 0.555^{i}	24.53 ± 0.57^{h}
KZL_7	7.34 ± 0.025^{ij}	22.97 ± 1.11^{i}
KZL_8	9.25 ± 0.025^{bc}	37.37 ± 0.62^{c}
KZL_9	9.48 ± 0.060^{a}	39.88 ± 0.21^{b}

Table 2. The WVP and WS values of KGM, zein, KZ, KZ films with different concentrations of LA and SA.

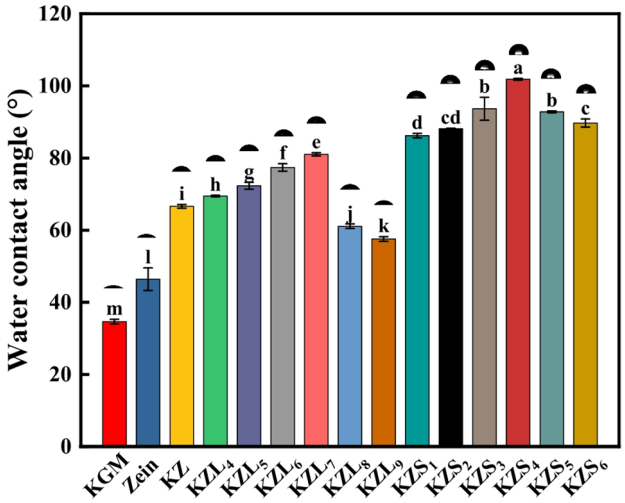

Fig. 7. Water contact angle of various films.

It was also observed from Table 2 that WS values showed similar trends as the WVP values. The WS value of pure KGM film was 90.08%, indicating that pure KGM film had strong hydrophilicity. The addition of zein significantly ($p < 0.05$) decreased the WS value of pure KGM film, suggesting that KZ film had better water resistance properties than pure KGM film. In addition, it was found that the WS values of KZ-FA films decreased first and then increased with the increase in FA concentrations. This was consistent with the water solubility of gelatin/gluten proteins films with palmitic acid in the literature[26]. Only KZL_8 and KZL_9 films were discovered to have higher WS values than KZ film, which meant that only KZL_8 and KZL_9 films had poorer water resistance properties than KZ film. KZS and KZL films had the lowest WS values when the concentrations of SA and LA were 0.4% and 0.07%, respectively. However, there was no much change in the WS value of KZ film among different types of fatty acids. More importantly, it was found that compared with other KGM-based films, KZS_4 film had the best water resistance properties. These results indicated that the water resistance properties of KZ film could be improved after adding fatty acids with appropriate concentrations.

Figure 7 shows the effects of fatty acids on the WCA value of KZ film. As seen from Fig. 7, the WCA value of pure KGM film was 34.64°, indicating that pure KGM film had poor hydrophobicity. Incorporating zein significantly ($p < 0.05$) increased the WCA value of pure KGM film, suggesting that KZ film had better hydrophobicity than pure KGM film, which may be due to the formation of hydrogen bonds between KGM and zein molecules. It was also observed that the WCA values of KZ-FA films increased first and then decreased with the increase of FA concentrations. Only KZL_8 and KZL_9 films were discovered to have lower WCA values than KZ film, which meant that only KZL_8 and KZL_9 films had weaker hydrophobicities than KZ film. KZS and KZL films had the highest WCA values when the concentrations of SA and LA were 0.4% and 0.07%, respectively. These results were in agreement with the WVP and WS values in this paper. However, KZS films had higher

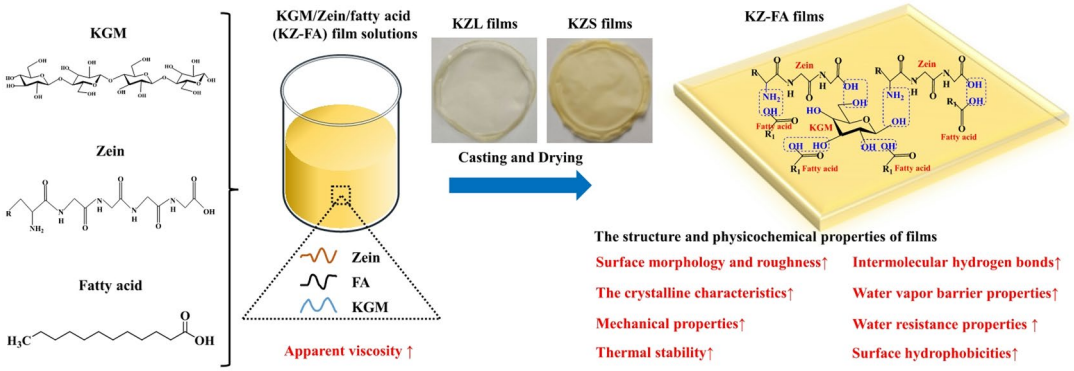

Fig. 8. The schematic diagram for the structure, physicochemical properties and underlying formation mechanism of KZ-FA films.

WCA values than KZ and KZL films, suggesting that KZS films exhibited stronger hydrophobicities than KZ and KZL films. Chen et al.[22] reported similar results that the addition of fatty acids significantly increased the contact angle values of soy protein isolate/sodium alginate film and the films with SA had higher hydrophobic characteristics. More importantly, it was found that compared with other KGM-based films, KZS_4 film had the highest surface hydrophobicity, which may be due to the strongest intermolecular interactions among KGM, zein, and SA at this unique blending ratio. These results indicated that adding SA to KZ film was beneficial to enhance the hydrophobicity.

It was well known that surface roughness is a key factor influencing contact angles. By observing the data of the contact angle and surface roughness, it was observed that except for KZS_4 film, there was a certain positive correlation trend between the contact angle of other KZS films and their surface roughness (SEM and AFM results). For KZS_4 film with low surface roughness, the wetting surface state may change, resulting in higher contact angle compared to KZS_3 film. In addition, beyond KZS_6 film, other KZS films were discovered to have higher contact angles than KZ and KZL films, presenting a certain positive correlation trend with their surface roughness. Moreover, except for KZL_4 and KZL_7 films, the contact angles of other KZL films were also found to show a certain positive correlation trend with their surface roughness. Therefore, it could be concluded that the contact angle results cannot be directly correlated with surface roughness data obtained from AFM and SEM analyses in this paper. This may be correlated to the experimental conditions, surface non-uniformity, physicochemical properties and multi-scale structure of different films.

Overall, the structure and physicochemical properties of KZ film were effectively improved after adding fatty acids. Moreover, the underlying formation mechanism of KZ-FA films was also proposed in this paper (Fig. 8). It was found that KGM, Zein, and fatty acids all had hydrogen bond interactions with each other, resulting in the formation of a more compact network structure. Therefore, this paper provides a novel idea for the preparation of hydrophobic KGM-based food packaging films with strong water resistance and water vapor barrier properties.

Conclusion

KGM/Zein/fatty acid (KZ-FA) films were successfully developed by a solution casting method and exhibited higher thermal stabilities and crystallinities than KZ film. The apparent viscosity of KZ film solution was significantly increased after incorporating fatty acids, and all the film-forming solutions exhibited the shear-thinning characteristics. In addition, hydrogen bond interactions among KGM, zein, and fatty acids occurred, resulting in the formation of a dense network structure demonstrated by microstructural analysis. Adding SA had a greater impact on the surface morphology and roughness of KZ film. The mechanical properties, surface hydrophobicity, water resistance and water vapor barrier properties of KZ film could be effectively enhanced after adding fatty acids with appropriate concentrations. The improved related properties enable KZ-FA films to be a great potential packaging material for the preservation of various foods, which may help to alleviate food safety and white environment pollution problems caused by conventional non-degradable petroleum-based packaging films. However, this article does not evaluate the stability of KZ-FA films in commercial applications and their preservation effects on different types of food. Therefore, further research will focus on optimizing the production processes of KZ-FA composite films through various advanced technologies and studying the practical applications of KZ-FA films in food packaging.

Data availability

All the data used and/or analyzed during the current study are available from the corresponding author on reasonable request.

Received: 4 November 2024; Accepted: 29 October 2025
Published online: 28 November 2025

References

1. Wu, Y. M., Wu, H. N. & Hu, L. D. Recent advances of proteins, polysaccharides and lipids-based edible films/coatings for food packaging applications: A review. *Food Biophys.* **19**, 29–45 (2024).
2. Sultan, M., Ibrahim, H., El-Masry, H. M. & Hassan, Y. R. Antimicrobial gelatin-based films with cinnamaldehyde and ZnO nanoparticles for sustainable food packaging. *Sci. Rep.* **14** (1), 22499 (2024).
3. Amin, U. et al. Potentials of polysaccharides, lipids and proteins in biodegradable food packaging applications. *Int. J. Biol. Macromol.* **183**, 2184–2198 (2021).
4. Mohamed, S. A. A., El-Sakhawy, M. & El-Sakhawy, M. A. M. Polysaccharides, protein and lipid-based natural edible films in food packaging: A review. *Carbohydr. Polym.* **238**, 116178 (2020).
5. Sarhadi, H., Shahdadi, F., Salehi Sardoei, A., Hatami, M. & Ghorbanpour, M. Investigation of physio-mechanical, antioxidant and antimicrobial properties of starch-zinc oxide nanoparticles active films reinforced with *Ferula gummosa* Boiss essential oil. *Sci. Rep.* **14** (1), 5789 (2024).
6. Xu, J. T. et al. Konjac glucomannan films with Pickering emulsion stabilized by TEMPO-oxidized Chitin nanocrystal for active food packaging. *Food Hydrocoll.* **139**, 108539 (2023).
7. Ni, Y. S. et al. Advanced Konjac glucomannan-based films in food packaging: Classification, preparation, formation mechanism and function. *LWT* **152**, 112338 (2021).
8. Wu, C. H. et al. Preparation and characterization of Konjac glucomannan-based Bionanocomposite film for active food packaging. *Food Hydrocoll.* **89**, 682–690 (2019).
9. Wang, S. C., Li, M. Y., He, B. B., Yong, Y. Y. & Zhu, J. Composite films of sodium alginate and Konjac glucomannan incorporated with tea polyphenols for food preservation. *Inter J. Biol. Macromol.* **242**, 124732 (2023).
10. Bu, N. T. et al. Konjac glucomannan/Pullulan films incorporated with cellulose nanofibrils-stabilized tea tree essential oil Pickering emulsions. *Colloids Surf. Physicochem Eng. Asp.* **650**, 129553 (2022).
11. Liu, Z., Lin, D. H., Lopez-Sanchez, P. & Yang, X. B. Characterizations of bacterial cellulose nanofibers reinforced edible films based on Konjac glucomannan. *Inter J. Biol. Macromol.* **145**, 634–645 (2020).
12. Zhang, W. & Rhim, J. W. Recent progress in Konjac glucomannan-based active food packaging films and property enhancement strategies. *Food Hydrocoll.* **128**, 107572 (2022).
13. Sun, J. S. et al. Multifunctional Bionanocomposite films based on Konjac glucomannan/chitosan with nano-ZnO and mulberry anthocyanin extract for active food packaging. *Food Hydrocoll.* **107**, 105942 (2020).
14. Qiao, D. L. et al. Zein inclusion changes the rheological, hydrophobic and mechanical properties of agar/konjac glucomannan based system. *Food Hydrocoll.* **137**, 108365 (2023).
15. Lan, X. et al. A review of food preservation based on zein: the perspective from application types of coating and film. *Food Chem.* **424**, 136403 (2023).
16. Li, Z. et al. Chitosan/zein films incorporated with essential oil nanoparticles and nanoemulsions: similarities and differences. *Inter J. Biol. Macromol.* **208**, 983–994 (2022).
17. Zhang, L. M. et al. The properties of chitosan/zein blend film and effect of film on quality of mushroom (*Agaricus bisporus*). *Postharvest Biol. Technol.* **155**, 47–56 (2019).
18. Li, C., Xiang, F., Wu, K., Jiang, F. T. & Ni, X. W. Changes in microstructure and rheological properties of Konjac glucomannan/zein blend film-forming solution during drying. *Carbohydr. Polym.* **250**, 116840 (2020).
19. Wang, L. et al. Characterization and antibacterial activity evaluation of Curcumin loaded Konjac glucomannan and Zein nanofibril films. *LWT* **113**, 108293 (2019).
20. Li, C. et al. Effect of drying temperature on structural and thermomechanical properties of Konjac glucomannan-zein blend films. *Inter J. Biol. Macromol.* **138**, 135–143 (2019).
21. Wang, K. et al. Structural characterization and properties of Konjac glucomannan and Zein blend films. *Inter J. Biol. Macromol.* **105**, 1096–1104 (2017).
22. Chen, H. et al. Effects of two fatty acids on soy protein isolate/sodium alginate edible films: structures and properties. *LWT* **159**, 113221 (2022).
23. Liu, P. F. et al. Effects of ultrasonication on the properties of maize starch/stearic acid/sodium carboxymethyl cellulose composite film. *Ultrason. Sonochem.* **72**, 105447 (2021).
24. Wu, X. N. et al. Effect of fatty acids with different chain lengths and degrees of unsaturation on film properties of potato starch-fatty acids films for chicken packaging. *Food Biophys.* **18**, 457–469 (2023).
25. Wang, R., Liu, P. F., Cui, B., Kang, X. M. & Yu, B. Effects of different treatment methods on properties of potato starch-lauric acid complex and potato starch-based films. *Inter J. Biol. Macromol.* **124**, 34–40 (2019).
26. Fakhouri, F. M. et al. The effect of fatty acids on the physicochemical properties of edible films composed of gelatin and gluten proteins. *LWT* **87**, 293–300 (2018).
27. Schmidt, V. C. R., Porto, L. M., Laurindo, J. B. & Menegalli, F. C. Water vapor barrier and mechanical properties of starch films containing stearic acid. *Ind. Crop Prod.* **41**, 227–234 (2013).
28. Akay, K. B., Başyiğit, B. & Karaaslan, M. Fatty-acid incorporation improves hydrophobicity of pea protein based films towards better oxygen/water barrier properties and fruit protecting ability. *Inter J. Biol. Macromol.* **276**, 133965 (2024).
29. Devi, L. S., Jaiswal, A. K. & Jaiswal, S. Lipid incorporated biopolymer based edible films and coatings in food packaging: A review. *Curr. Res. Food Sci.* **8**, 100720 (2024).
30. Xu, X. Y. et al. Performance enhancing of saturated fatty acids with various carbon chain lengths on the structures and properties of Zein films in alkaline solvents. *Food Hydrocoll.* **155**, 110214 (2024).
31. Zhou, F. et al. Preparation, characterization and application of Konjac glucomannan/pullulan/microcrystalline cellulose/tea polyphenol active blend film. *Food Biosci.* **49**, 101898 (2022).
32. Du, Y. et al. Fabrication of novel Konjac glucomannan/shellac film with advanced functions for food packaging. *Inter J. Biol. Macromol.* **131**, 36–42 (2019).
33. Xiang, F. et al. Preparation of Konjac glucomannan based films reinforced with nanoparticles and its effect on Cherry tomatoes preservation. *Food Packag Shelf Life.* **29**, 100701 (2021).
34. Wang, Y. F., Yu, L., Sun, Q. J. & Xie, F. W. Hydroxypropyl Methylcellulose and hydroxypropyl starch: rheological and gelation effects on the phase structure of their mixed hydrocolloid system. *Food Hydrocoll.* **115**, 106598 (2021).
35. Wang, Q., Song, Y. Y., Sun, J. & Jiang, G. A novel functionalized food packaging film with microwave-modified Konjac glucomannan/chitosan/citric acid incorporated with antioxidant of bamboo leaves. *LWT* **166**, 113780 (2022).
36. Wang, M. et al. Effect of honeysuckle leaf extract on the physicochemical properties of carboxymethyl Konjac glucomannan/konjac glucomannan/gelatin composite edible film. *Food Chem. X.* **18**, 100675 (2023).
37. Lin, W. M., Ni, Y. S. & Pang, J. Microfluidic spinning of Poly (methyl methacrylate)/konjac glucomannan active food packaging films based on hydrophilic/hydrophobic strategy. *Carbohydr. Polym.* **222**, 114986 (2019).
38. Ni, Y. S. et al. Facile fabrication of novel Konjac glucomannan films with antibacterial properties via microfluidic spinning strategy. *Carbohydr. Polym.* **208**, 469–476 (2019).
39. Zhang, L. M. et al. Chitosan/zein bilayer films with one-way water barrier characteristic: Physical, structural and thermal properties. *Inter J. Biol. Macromol.* **200**, 378–387 (2022).
40. García, M. A., Martino, M. N. & Zaritzky, N. E. Lipid addition to improve barrier properties of edible starch-based films and coatings. *J. Food Sci.* **65**, 941–947 (2000).

41. Jim´enez, A., Fabra, M. J., Talens, P. & Chiralt, A. Phase transitions in starch based films containing fatty acids. Effect on water sorption and mechanical behavior. *Food Hydrocoll.* **30**, 408–418 (2013).
42. De la Caba, K. et al. Characterization of soybean protein concentrate-stearic acid/palmitic acid blend edible films. *J. Appl. Polym. Sci.* **124**, 1796–1807 (2012).
43. Wang, L., Lin, L. Z., Chen, X. H., Tong, C. L. & Pang, J. Synthesis and characteristics of Konjac glucomannan films incorporated with functionalized microcrystalline cellulose. *Colloids Surf. Physicochem Eng. Asp.* **563**, 237–245 (2019).
44. Gahruie, H. H. et al. The effects of fatty acids chain length on the techno-functional properties of Basil seed gum-based edible films. *Inter J. Biol. Macromol.* **160**, 245–251 (2020).
45. Zahedi, Y., Ghanbarzadeh, B. & Sedaghat, N. Physical properties of edible emulsified films based on pistachio Globulin protein and fatty acids. *J. Food Eng.* **100**, 102–108 (2010).
46. Cheng, Y. et al. Effect of lipids with different physical state on the physicochemical properties of starch/gelatin edible films prepared by extrusion blowing. *Inter J. Biol. Macromol.* **185**, 1005–1014 (2021).
47. Galus, S. Functional properties of soy protein isolate edible films as affected by rapeseed oil concentration. *Food Hydrocoll.* **85**, 233–241 (2018).
48. Wang, Y. Y., Liu, F. G., Liang, C. X., Yuan, F. & Gao, Y. X. Effect of Maillard reaction products on the physical and antimicrobial properties of edible films based on ε-polylysine and Chitosan. *J. Sci. Food Agr.* **94**, 2986–2991 (2014).

Acknowledgements

This work was supported by Natural Science Foundation of Fujian Province (2024J01879, 2021J011105, 2020J05211), Science and Technology Department of Putian (2018NP2003), Research Projects of Putian University (2024035).

Author contributions

Xiumei Wang: Conceptualization, Methodology, Writing-original draft. Xiaoyan Zheng: Investigation, Validation. Leqian Chu: Investigation, Validation. Xiaoxu Zhao: Supervision, Data Curation, Writing-Review & Editing. Jie Pang: Conceptualization, Supervision, Writing-Review & Editing.

Declarations

Competing interests

The authors declare no competing interests.

Additional information

Correspondence and requests for materials should be addressed to X.Z. or J.P.

Reprints and permissions information is available at www.nature.com/reprints.

Publisher's note Springer Nature remains neutral with regard to jurisdictional claims in published maps and institutional affiliations.